



Cite this: *Dalton Trans.*, 2016, **45**, 1166

Colorimetric detection of fluoride ions by anthraimidazoledione based sensors in the presence of Cu(II) ions†

Amrita Sarkar, Sudipta Bhattacharyya and Arindam Mukherjee*

Anthraquinone based anion receptors have gained importance due to their colorimetric response on sensing a specific anion and the possibility of tuning this property by varying the conjugated moiety (the donor) to the diamine. In this work, we have synthesized and characterized four anthraimidazoledione compounds having 2,5-dihydroxy benzene, 4-(bis(2-chloroethyl)amino)benzene, imidazole and 4-methylthiazole moieties respectively (**1–4**). All of them were probed for their potential as anion sensors to study the effect of changes in the hydrogen bond donor–acceptor. The *p*-hydroquinone bound anthraimidazoledione (**1**) and thioimidazole bound anthraimidazoledione (**4**) were able to detect both F[−] and CN[−] in the presence of other anions Cl[−], Br[−], I[−], H₂PO₄[−], OAc[−], NO₃[−] and ClO₄[−]. Both **1** and **4** could not differentiate F[−] from CN[−] and provided a similar response to both. The ¹H NMR studies of **1** and **4** with F[−], showed the formation of [HF₂][−] at 16.3 ppm and the ¹⁹F NMR showed a sharp peak at −145 ppm in both cases. However, although there may be NMR evidence of [HF₂][−] formation F[−] may not be detected colorimetrically if the CT band remains almost unchanged, as found for **3**. The results emphasize that the change of a hetero atom in the donor moiety of an anthraimidazoledione may render a large difference in sensitivity. In the case of **4** selective detection of F[−] was possible in the presence of 0.5 equivalent of Cu²⁺ with the exhibition of a distinct green colour with a $\Delta\lambda$ shift of ca. 50 nm in contrast to CN[−] which showed orange colouration with a $\Delta\lambda$ shift of only 15 nm. In the presence of Cu²⁺ the F[−] detection limit was 0.038(5) ppm (below the WHO specified level) at a receptor concentration of 25 μ M.

Received 19th August 2015,
Accepted 30th November 2015

DOI: 10.1039/c5dt03209a

www.rsc.org/dalton

Introduction

Anion sensing has become a popular area of research due to its potential role in various biological processes and in environmental chemistry.^{1–6} The well-known advantages of a highly sensitive and selective anion sensor have led to a surge in research in this area, especially in the past decade.^{7,8} Among various anionic analytes fluoride and cyanide seem to be of potential interest for their established roles in physiology.⁹ The benefits of fluoride are well known in the treatments of osteoporosis, orthodontics, enamel demineralisation and as anti-depressants.¹⁰ However, the excessive intake of fluoride often leads to fluorosis,^{11–13} urolithiasis^{9,14} and even cancer.^{9,15} Cyanide the extremely toxic anion for mammals has extensive industrial applications including gold mining, electroplating,

metallurgy, paper, textile and plastic industries.¹⁶ The wide range use of cyanide may also be a major cause of contamination of various environmental sources spiking the cyanide amount beyond the safe limit. It is well known that cyanide inhibits cellular respiration by strong interactions with cytochrome a_3 of the heme unit.¹⁷ A very small amount of cyanide can be lethal to various metabolic functions including cardiac, renal, vascular, respiratory and central nervous systems.¹⁸

Hence contamination of water sources with cyanide and fluoride is a matter of concern.¹⁹ According to World Health Organisation (WHO) and Environment Protection Agency (EPA) the permissible level of fluoride and cyanide in drinking water should be 1.5 and 0.2 ppm respectively.²⁰ Therefore, various methods have been developed for the detection of fluoride and cyanide among which colorimetric sensors have gained much importance due to their straight forward ‘naked-eye’ detection ability allowing them to be an inexpensive detection technique.^{2,21–34}

Three main approaches have been used to develop various anion sensors:

(i) anion binding to the hydrogen bond donor site due to which the electronic properties of the receptor is altered allowing the subsequent detection of anions.^{5,30,35–46}

Department of Chemical Sciences, Indian Institute of Science Education and Research Kolkata, Mohanpur 741246, India. E-mail: a.mukherjee@iiserkol.ac.in; Fax: +91-33-25873020

† Electronic supplementary information (ESI) available: Detailed UV-vis spectral data, fitting plots, ¹H, ¹⁹F NMR titration data, ¹H and ¹³C NMR characterization data. See DOI: [10.1039/c5dt03209a](https://doi.org/10.1039/c5dt03209a)



(ii) Displacement assay, which involves the formation of a complex between an indicator ion and a receptor, followed by the displacement of the indicator by guest anions.^{47–56} This creates a change in the microenvironment of the receptor resulting in alteration in colours or fluorescence properties.^{55,56,57}

(iii) Generation of new species with different properties upon chemical reaction between anionic species and receptor molecules called chemodosimeters.^{58–63}

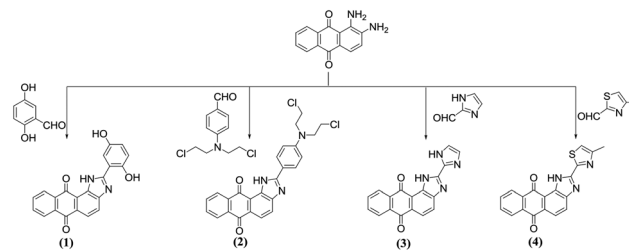
The hydrogen bond donating receptors include a wide range of molecules *viz.* ureas,^{35,64,65} thioureas,^{44,66–68} imidazoles/benzimidazoles,^{21,45,69–75} amides/diamides,^{76–78} indolocarbazoles,^{30,79,80} guanidinium derivatives,⁸¹ azophenol,^{31,82} naphthalimides,^{83–87} pyrrole,^{88,89} callixpyrrole^{90–93} etc. The benzimidazole derivatives work *via* the deprotonation of N–H groups which results in either fluorescence quenching,^{45,94} photoinduced electron transfer (PET)^{95–97} or intramolecular charge transfer (ICT) processes.^{21,75,98} The ICT process involves a ‘push–pull’ mechanism between a donor (D) and an acceptor (A) moiety and binding of the negatively charged analyte to the electron deficient acceptor (A) moieties modulates the charge transfer character of the D–A system.^{21,99,100} In colorimetric anthraquinone-imidazole based receptors the charge transfer band arises mainly from the $\pi_{\text{imidazole}} \rightarrow \pi_{\text{anthraquinone}^*}$ electronic transition.^{20,21,34,97} Compounds **1** and **4** were found to be sensitive towards F^- and CN^- as per the results of UV-vis spectroscopic studies. However, **2** and **3** did not show any recognition capability in the presence of the above-mentioned anion using the same receptor concentration as **1** and **4** (*i.e.* 25 μM) (Fig. S2 and S3, ESI[†]).

In this work, we varied the donor system with different aromatic systems including 2,5-dihydroxy benzene, 4-(bis(2-chloroethyl)amino)benzene, imidazole and 4-methylthiazole to prepare four compounds with potential as chemosensors (**1–4**). Our objective was to study how the variation of the donor type changes the compounds’ behaviour towards the anions of choice *viz.* fluoride and cyanide. Our endeavour showed that among compounds **1–4**, compounds **1** and **4** detect F^- and CN^- with an almost similar efficiency but could not exhibit any difference in recognition between F^- and CN^- separately. However, in the presence of Cu^{2+} **4** could distinguish F^- from CN^- and hence compound **4** can act as a receptor for recognition of F^- with a detection limit of 0.038(5) ppm at a receptor concentration of 25 μM .

Results and discussion

Syntheses

We have synthesized four anthraimidazoledione derivatives (**1–4**) with four different aldehydes as depicted in Scheme 1. All the compounds were well characterized by ^1H NMR, ^{13}C NMR, CHN, IR as well as ESI-MS. The data obtained confirm the purity of the compounds. All compounds presented here are soluble in $\text{DMSO}-d_6$. The compounds are not soluble in any chlorinated solvent. Their solubility in polar protic solvents is good enough for the electronic spectral studies and anion recognition. All the compounds are insoluble in water.



Scheme 1 Representative synthetic scheme for the preparation of **1–4**. Reaction conditions applied: ethanol (100 mL), trifluoroacetic acid (catalytic amount), heated to reflux for 16–18 h.

Anion recognition without Cu^{2+} ions: colorimetry and spectrophotometry. The anion recognition properties of all the synthesized compounds were probed in an acetonitrile and DMSO mixture (40 : 1) with the addition of various anions (F^- , Cl^- , Br^- , I^- , CN^- , NO_3^- , H_2PO_4^- , OAc^- and ClO_4^-) as tetrabutylammonium salts. Water was avoided due to poor solubility of the receptors. All of the four compounds exhibit a charge transfer band around 409–499 nm (Fig. S1, ESI[†]), which may be assigned to the $\pi_{\text{imidazole}} \rightarrow \pi_{\text{anthraquinone}^*}$ electronic transition.^{20,21,34,97} Compounds **1** and **4** were found to be sensitive towards F^- and CN^- as per the results of UV-vis spectroscopic studies. However, **2** and **3** did not show any recognition capability in the presence of the above-mentioned anion using the same receptor concentration as **1** and **4** (*i.e.* 25 μM) (Fig. S2 and S3, ESI[†]).

The use of 25 μM of **1** and **4** showed that the ICT bands were red-shifted upon gradual addition of F^- and CN^- in contrast to other anions. Compound **1** has the 2,5-dihydroxy substituted aryl ring as the donor and anthraquinone as the acceptor. **1** showed a positive but similar colorimetric response in the presence of either F^- or CN^- . It did not respond to other afore-mentioned common anions probed here (Fig. 1). The

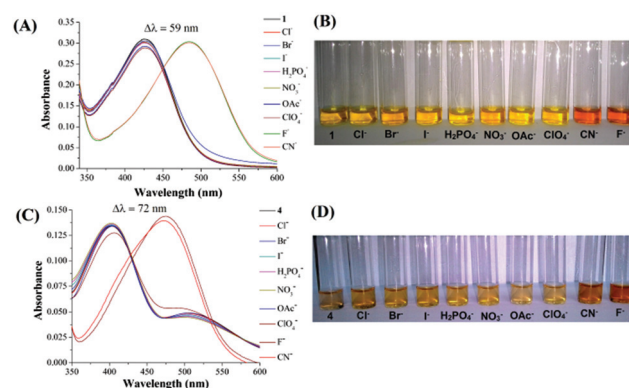


Fig. 1 (A) UV-vis of **1** (25 μM) in acetonitrile (2.5% DMSO) after addition of 6 equivalent anions, (B) colorimetric response of **1** in the presence of different anions (6 equivalents), (C) UV-vis of **4** (25 μM) in acetonitrile (2.5% DMSO) after addition of 6 equivalent anions, (D) colorimetric response of **4** in the presence of different anions (6 equivalents).

colour of the solution turned from yellow to bright orange when F^- and CN^- solutions were added to the solution of **1** (ACN:DMSO = 40:1) (Fig. 1). The charge transfer band at 425 nm showed a bathochromic or red shift ($\Delta\lambda = 59$ nm) for both F^- and CN^- .

When **4** was used as the sensor the red shift of the band at 400 nm was more for both CN^- ($\Delta\lambda = 68$ nm) and F^- ($\Delta\lambda = 72$ nm) compared to **1**. The successive addition of F^- and CN^- ions to **1** showed a gradual decrease in the absorption band at 425 nm and increase at 484 nm. The saturation limits were achieved with the addition of 1.6 equivalents of F^- and 1.4 equivalents of CN^- ions. The titration curves for F^- and CN^- ions are shown in Fig. 2. Successive addition of F^- or CN^- solution to **4** showed a gradual decrease in absorbance in the range of 401–404 nm along with a concomitant increase in the range of 472–474 nm (Fig. 3). The saturation limit was achieved much earlier for CN^- (1.28 equiv., 32 μM) compared to F^- (2.48 equiv., 62 μM). The saturation achieved with low excess of the anions suggests that the sensitivity is high towards F^- or CN^- . The presence of isosbestic points, at 450 nm for **1** (Fig. 2) and 430 nm for **4** (Fig. 3), in the case of either F^- or CN^- , indicates the presence of two different species at equilibrium. The presence of two different isosbestic points at 350 and 450 nm for **1** and 345 and 430 nm for **4** suggests that the binding stoichiometry may be 1:1. Hence we performed a Job's plot for receptors **1** and **4** with F^- and CN^- and confirmed that the binding ratio is 1:1 (Fig. 4). The data showed that both **1** and **4** are not able to distinguish between F^- or CN^- and detect both of them. The above results signify that both F^- and CN^- are almost equally efficient in forming adducts with the $-\text{NH}$ proton in **1** and **4** thereby leading to the deprotonation of $-\text{NH}$ and decreasing the energy gap between the $\pi_{\text{imidazole}}$ and $\pi_{\text{anthraquinone}}^*$ orbitals rendering a bathochromic shift.

As mentioned earlier **3**, where two imidazole rings are present, did not show anion recognition in the same receptor

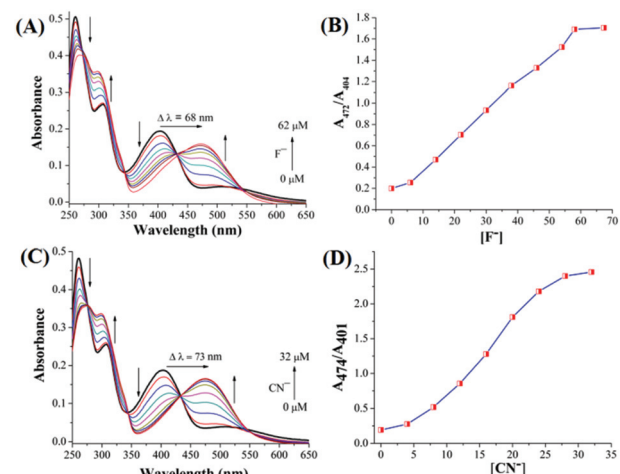


Fig. 3 UV-vis spectroscopic titration of **4** (25 μM) with (A) fluoride (0–62 μM), (B) ratiometric plot with fluoride, (C) cyanide (0–32 μM) and (D) ratiometric plot with cyanide.

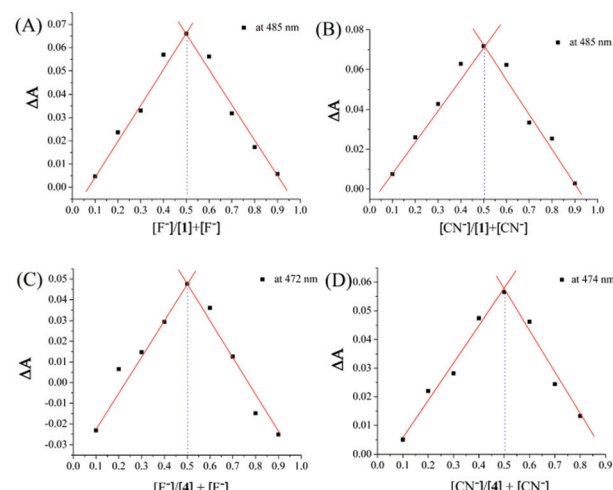


Fig. 4 Job's plot of receptors **1** and **4** where absorbances at 484 nm (for **1**) and at 472–474 nm (for **4**) were plotted as a function of the molar ratio of **1** and **4**. (A) **1** with F^- , (B) **1** with CN^- , (C) **4** with F^- and (D) **4** with CN^- .

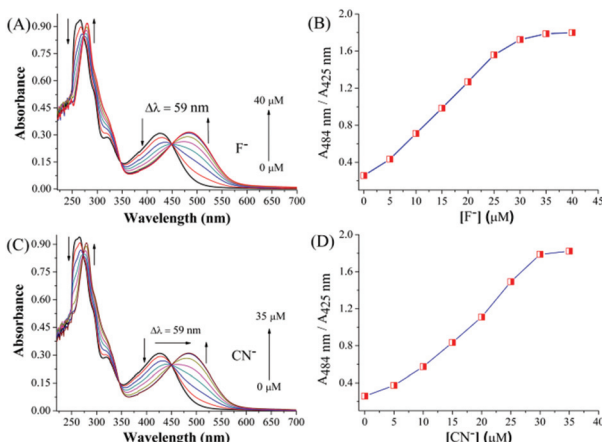


Fig. 2 UV-vis spectroscopic titration of **1** (25 μM) with (A) fluoride (0–40 μM), (B) ratiometric plot with fluoride, (C) cyanide (0–35 μM) and (D) ratiometric plot with cyanide.



spectrum reverted to its original position (Fig. S5A, ESI†). The results signify that the deprotonation of the imidazole hydrogen of **3** is difficult compared to **1** and **4** and it also corroborates well since in the presence of a base the colour change of the CT band takes place but after a while reverts to original. We probed the behaviour of **3** with F^- and found that it is less sensitive to the addition of F^- when compared with **1** and **4** and takes at least 110 equivalents of F^- to achieve a similar 50 nm shift, which is saturated at 230 equivalents of F^- (Fig. S5B, ESI†). The above phenomenon leads to a poor detection limit of F^- by **3** (259 mM; 1054 ppm). In the case of **2** the presence of the weak electron withdrawing bis(2-chloroethylamine) moiety decreases the acidity of the imidazole proton hence the F^- or the CN^- adduct is weaker and unstable and **2** is not suitable for use as a sensor of the probed anions.

The obtained differences in the results based on the addition of TBAOH and TBAF/TBACN suggest the use of TBAOH for mechanistic purpose may be useful but the receptors may be much less sensitive to the anions *viz.* F^- and CN^- compared to the deprotonation by OH^- and hence the predicted mechanism is only an indication of the possible pathway. The binding stoichiometry for the receptors **1** and **4** was evaluated using the Job's plot and it was found that they bind in a 1 : 1 ratio as shown in Fig. 4.

We calculated the detectable limit of fluoride and cyanide ions from the ratiometric plot of $A_{484\text{nm}}/A_{425\text{nm}}$ *vs.* [anion].¹⁰⁷ The apparent association constants for anions were calculated from nonlinear regression analysis and the values are tabulated in Table 1. The apparent binding constants for F^- and CN^- are in the range of 10^3 to 10^4 M^{-1} showing relatively weak binding with the anions. The association constants in Table 1 show that without the influence of Cu^{2+} , CN^- has a higher affinity for receptors **1** and **4** signifying that under such conditions CN^- is more efficient in deprotonating the $-\text{NH}$. The UV-vis titrations also show that less CN^- is required to achieve saturation compared to the amount of F^- . The detection limits were calculated in parts per million (ppm) units. The calculations show that the detection limits are lower than the permitted limit set by WHO or EPA for both fluoride (1.5 ppm) and cyanides (0.2 ppm).^{20,108} We achieved the lowest detection limit of *ca.* 0.07(6) ppm for F^- in the case of **1** and 0.12(3) ppm for CN^- in the case of **4**. However, it should be noted that **1** and **4** could not distinguish CN^- from F^- but we will see later that the presence of Cu^{2+} helps the selective detection of F^- .

Table 1 Apparent binding constants for **1** and **4**^a

Receptors	Anions	$\Delta\lambda$ (nm)	K_{asso} (M^{-1})	Detection limit (ppm)
1	F^-	59	$5.63(8) \times 10^3$	0.068(6)
	CN^-	59	$1.27(3) \times 10^4$	0.164(4)
4	F^-	68	$1.17(2) \times 10^4$	0.081(2)
	CN^-	73	$4.9(3) \times 10^4$	0.123(3)

^a Experiments were carried out in triplicate. The values in parentheses show standard errors.

1H titration experiment

The mechanism of F^- and CN^- detection was further explored through NMR using ^1H NMR titration experiments for the receptors **1** and **4** in $\text{DMSO}-d_6$. With the addition of TBAF solution to **1** we observed that the two singlet peaks at 12.7 and 11.2 ppm for the two phenolic $-\text{OH}$ vanished signifying quick chemical exchange or possible deprotonation in the presence of the anion and the singlet NH peak at 9.2 ppm was also broadened (Fig. 5). The broadening of the NH peak suggests that the imidazole hydrogen may be experiencing hydrogen bonding interactions with F^- . After the addition of 1.0 equivalent of TBAF the imidazole N-H signal vanished emphasizing that the F^- might have deprotonated the $-\text{NH}$ group by interactions with the hydrogen trying to form the $[\text{HF}_2]^-$ type of species. Indeed after the addition of 2.5 equivalents of F^- one triplet started to appear at *ca.* 16.3 ppm which is known to be due to the formation of the adduct $[\text{HF}_2]^-$ (Fig. 5). This adduct formation was also confirmed by ^{19}F NMR where we observed a sharp peak around -145 ppm for this same adduct formation (Fig. S6†).¹⁰⁹ The deprotonation of imidazole $-\text{NH}$ develops a negatively charged ring causing the upfield shift of protons of the anthraquinone moiety. Beside the triplet peak at 16.3 ppm for the $[\text{HF}_2]^-$ adduct, one singlet peak at 14.5 ppm gradually increases at the same time and generation of this singlet peak might be due to the formation of $[\text{N}^{\delta-}\cdots\text{H}^{\delta+}\cdots\text{O}^{\delta-}]$ as shown in Fig. 5 since if it was due to the formation of $[\text{O}^{\delta-}\cdots\text{H}^{\delta+}\cdots\text{F}^{\delta-}]$ then it should have appeared as a doublet instead of a singlet, but we only observed a singlet in the spectra (Fig. 5, inset A) which agrees well with similar observations in the literature.¹¹⁰ This peak of $[\text{N}^{\delta-}\cdots\text{H}^{\delta+}\cdots\text{O}^{\delta-}]$ arises due to the hydrogen bonding of an imidazole nitrogen with one of the $-\text{OH}$ groups of the hydroquinone upon deprotonation of the $-\text{NH}$ in the imidazole ring.

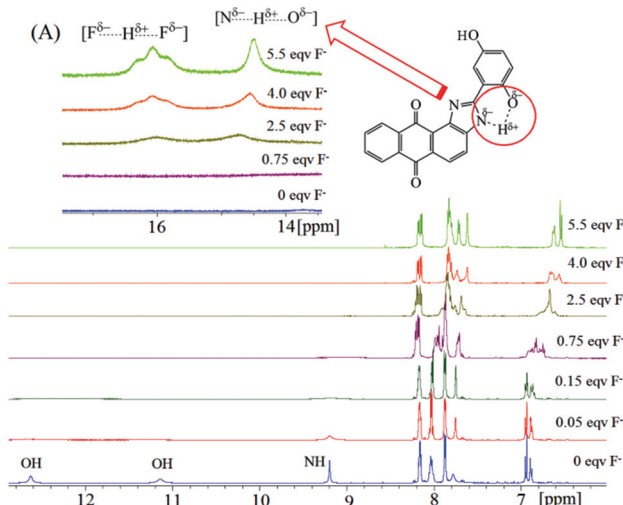


Fig. 5 Partial ^1H NMR spectra of **1** ($4.96 \times 10^{-2} \text{ M}$) in $\text{DMSO}-d_6$ in the presence of TBAF (0–5.5 equivalents). Inset: (A) expansion of the region 14–17 ppm in the presence of 2.5–5.5 equivalents of TBAF.

Compound **4** also showed the generation of a triplet peak for $[\text{HF}_2]^-$ at *ca.* 16.3 ppm with the successive addition of TBAF in the ^1H NMR (Fig. S7, inset A, ESI \dagger). The imidazole -NH peak at 7.9 ppm also broadened and ultimately vanished after the addition of 1.25 equivalents of F^- . The ^{19}F NMR also confirms the deprotonation since we observed a sharp peak at *ca.* -145 ppm for the $[\text{HF}_2]^-$ adduct formation (Fig. S8, ESI \dagger). The deprotonation phenomenon was further confirmed from the results of the UV-vis experiment of **1** and **4** with a strong base *viz.* TBAOH. We observe a similar red shift of *ca.* 57 nm and 72 nm respectively (Fig. S9, ESI \dagger) comparable to that obtained for F^- and CN^- using the same receptors.

To study the effect of cyanide addition, ^1H NMR titrations were performed with **1** and **4** with TBACN. We could observe the -NH and -OH signals vanishing upon addition of 0.4–1.0 equivalents of TBACN for both **1** and **4** (Fig. S10, S11 \dagger) and the same colour change suggests speciation similar to F^- for receptors **1** and **4**. Hence, the electronic spectroscopy studies could not distinguish between the fluoride and cyanide.

We also probed ^1H and ^{19}F titration for **3** using 5.4×10^{-2} M receptor concentration which is close to that taken for the NMR studies of **1** and **4** (4.96×10^{-2} M for **1** and 9.9×10^{-2} M for **4**). We observed deprotonation of the imidazole hydrogen and the formation of the $[\text{HF}_2]^-$ adduct both in ^1H (triplet at *ca.* 16.1 ppm) and ^{19}F NMR (doublet at *ca.* -143 ppm) (Fig. S12–S14 \dagger). However, as mentioned earlier there is no F^- recognition by **3** at concentrations similar to **1** and **4** and even at higher concentrations (1.4×10^{-3} M) and at least 110 equivalent excess concentration of F^- is required for recognition (Fig. S5B, ESI \dagger).

In order to achieve a recognizable difference in the UV-vis spectra due to changes in the interaction we used Cu^{2+} . Since Cu^{2+} is known to have a stronger interaction with CN^- we thought that this will help us based on the numerous literature reports available with Cu^{2+} enabling cyanide sensing in the presence of a ligand.^{56,111–114} When we probed, we found that instead of cyanide the F^- sensing improved in the presence of Cu^{2+} as discussed in the next section.

In the presence of Cu^{2+} ions

The spectral pattern of the CT band in **4** in the presence of Cu^{2+} showed a distinct effect and we could achieve specific recognition of F^- . The successive addition of F^- and CN^- ions to **4** in the presence of 0.5 equivalent of Cu^{2+} is displayed in Fig. 6. We have added up to 60 μM (2.4 equivalents) of CN^- to obtain only a 15 nm red shift. We did not find the 15 nm shift in the presence of CN^- to be sufficient for a good detection so we did not attempt studies on detection of cyanide with **4**. The change in $\Delta\lambda$ for F^- showed a difference of 50 nm compared to that of *ca.* 15 nm for CN^- (Fig. 6 and Fig. S15, ESI \dagger). On addition of approx. half equivalent of Cu^{2+} with respect to sensor **4**, the yellow solution turns orange for all the anions probed except for F^- . Addition of up to *ca.* 5.6 equivalents of Cu^{2+} alone did not render any considerable change in the CT band ($\lambda_{\text{max}} = 400$ nm) (Fig. S16A, ESI \dagger). However, in the pres-

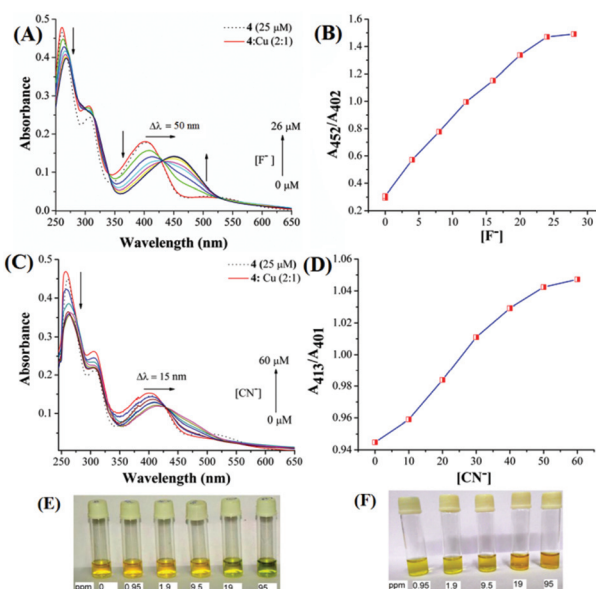


Fig. 6 UV-vis spectroscopic titration of **4** (25 μM) with (A) fluoride (0–26 μM), (B) ratiometric plot with fluoride, (C) cyanide (0–60 μM) and (D) ratiometric plot with cyanide. (E) Colorimetric response of **4** (25 μM) in the presence of Cu^{2+} (12.5 μM) with the addition of different concentrations of fluoride solution. (F) Visual colorimetric response of **4** (25 μM) in the presence of Cu^{2+} (12.5 μM) with the addition of different concentrations of cyanide solution. (Fluoride and cyanide solution: 0.95, 1.9, 9.5, 19 and 95 ppm.)

ence of only 0.5 equivalent Cu^{2+} **4** could sense F^- specifically as the CT band shifts by 50 nm.

In order to probe if deprotonation is one of the causes for recognition even in the presence of Cu^{2+} , we carried out UV-vis titration with up to *ca.* 1.2 equivalents of TBAOH instead of 1 equivalent of F^- . A similar 51 nm red shift was observed. The above data suggest that the deprotonation phenomenon is also acting in the presence of Cu^{2+} ions (Fig. S16B, ESI \dagger). The Job's plot for F^- sensing for **4** in the presence of Cu^{2+} also indicates a 1 : 1 ratio (Fig. S17, ESI \dagger). Comparatively **1** hardly showed any significant change usable for detection purpose by a shift in the charge transfer band on addition of the other afore-mentioned anions in the presence of Cu^{2+} (Fig. S18 and S19, ESI \dagger).

We found that with the successive addition of F^- to **4** in the presence of Cu^{2+} a gradual decrease in the absorption band at 401 nm was observed with a concomitant increase at 451 nm. The saturation limits were achieved with addition of just 1 equivalent of F^- . The apparent association constant of **4** for F^- and CN^- in the presence of Cu^{2+} was found to be $1.37(2) \times 10^5 \text{ M}^{-1}$ and the detection limit was achieved to be 0.038(5) ppm in the case of F^- (Table 2).

Compounds **1–4** have anthraquinone in common but the pendant moieties attached to the imidazole ring fused with anthraquinone are different. We found that **2** and **3** do not exhibit distinct recognition for any of the probed anions but **1** and **4** recognize F^- and CN^- . In the case of **1** the proton of the imidazole moiety is released in the presence of F^- and CN^- which renders a spectral change leading to the recognition of



Table 2 Apparent binding constants for **4** in the presence of Cu^{2+} ^a

Receptor	Anions	$\Delta\lambda$ (nm)	K_{asso} (M^{-1})	Detection limit (ppm)
4	F^-	50	$1.37(2) \times 10^5$	0.038(5)
	CN^-	15	$1.19(4) \times 10^4$	0.237(3)

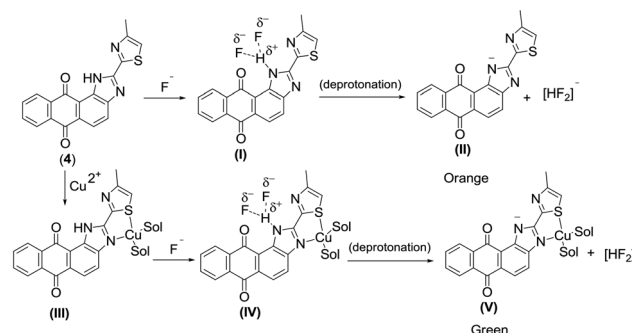
^a Experiments were carried out in triplicate. The values in parentheses show standard errors.

the fluoride or cyanide. Since both F^- and CN^- are equally efficient in interacting with the proton of the imidazole they cannot be distinguished from each other by **1**.

The titration experiments of **1–4** with OH^- show that **4** is the easiest one to deprotonate as seen from the UV spectral changes (Fig. S20D, ESI†) followed by **1** (Fig. S20A, ESI†) which is also pretty similar in terms of stoichiometry needed to observe the change in the CT band which may be assigned to the deprotonation of the benzimidazole nitrogen. Compounds **2** and **3** however require higher stoichiometries of OH^- to observe the bathochromic shift of the CT band as seen in Fig. S20B & C, (ESI†). Receptor **2** requires at least 9 molar equivalents of OH^- to initiate the prominent spectral change of the CT band and **3** requires at least 7 molar equivalents of OH^- for the same (Fig. S20B and C, ESI†). In contrast for **1** and **4** the saturation for the shift in the charge transfer band is achieved within 1.0 molar equivalent of OH^- . The above results signify that the benzimidazole $-\text{NH}$ has low acidity in **2** and **3** compared to **1** and **4**. Hence, **2** and **3** are not useful as sensors to recognize any of the probed anions including F^- and CN^- .

The NMR studies showed that HF_2^- is formed in **3** similar to that reported in the literature and found by us for **1** and **4**. However, the NMR studies are performed in greater concentrations and prominent changes are observed with higher equivalents of F^- compared to the UV-vis studies. Hence, the formation of HF_2^- should not be considered as a sufficient indication. Hence the visible colour change to the CT band, rendered by the interaction of the anion to the receptor is necessary for the recognition which is also dependent on the acidity of the $-\text{NH}$ proton. The presence of the sulphur atom in **4** is clearly advantageous to render the colour change of the CT band upon interaction of the F^- with **4** since it helps the recognition with Cu^{2+} . The presence of Cu^{2+} should lead to an interaction between the receptor and the Cu^{2+} although we did not observe any colour change upon addition of Cu^{2+} to the receptor **1** or **4** (Fig. 6 and S16A, S19A, ESI†) but in the presence of F^- and Cu^{2+} in the case of **4** the change becomes significant which is in contrast to other anions including CN^- .

In most cases the probable species formed which renders the colour is not commented on since it is understood that the uncertainties are high. However, based on the evidence obtained we propose a plausible speciation for the F^- detection by **4** (Scheme 2). We strongly feel that prediction of the possible interactions would lead to better understanding of the possible species responsible for recognition in future. The

**Scheme 2** Mechanistic proposal of fluoride sensing by **4** in the absence and in the presence of Cu^{2+} .

above speciation is based on the following: (i) we have seen that in the presence of TBAOH and in the presence of F^- the colour change is the same using similar concentrations of the anions. Hence, deprotonation may be occurring in both cases leading to the formation of HF_2^- which supports that species **II** may be forming in solution rendering the colouration. (ii) The position of HF_2^- is almost the same in both the cases of **1** and **4** suggesting that they may not be influenced by other atoms of **1** and **4** i.e. the formed HF_2^- may be independent from the negatively charged receptor molecule and helps recognition supporting the formation of **II** (Scheme 2). (iii) In the presence of Cu^{2+} added to the solution of **1** or **4** we do not see much shift in the native CT-band but when F^- is added to **4** there is a similar shift to that observed in the presence of TBAOH and Cu^{2+} . Hence here **V** may be the species forming in solution rendering the colouration. The small shift of 15 nm for the CT band in the case of addition of CN^- in the presence of Cu^{2+} shows that the interaction of CN^- in the presence of Cu^{2+} is weaker than F^- which is supported by the obtained association constant (Table 2). Based on the results, **4** is not suitable for CN^- recognition.

The structural difference of receptor **1** renders a different speciation in the presence of Cu^{2+} , which does not increase the acidity of the $-\text{NH}$ proton of the benzimidazole sufficient enough such that it may be deprotonated by F^- or CN^- . However, due to the stronger deprotonation ability of TBAOH the CT band of **1** shows a shift (Fig. S16 and S19, ESI†) similar to that in the case of **4** (in the presence of F^- and Cu^{2+}). The data also show that a higher concentration of OH^- is required in **1** to observe changes in the CT band similar to **4** suggesting that the F^- may not be able to form the anion of **1** diminishing its recognition capability.

Our preliminary computational studies by the DFT level of theory with the B3LYP function and 6-31G(d) basis set showed that the charge transfer bands are indeed from $\pi_{\text{imidazole}} \rightarrow \pi_{\text{anthraquinone}^*}$ (Fig. S21 and Table S1, ESI†) as assigned earlier in the literature,^{20,21,34,97} and the bathochromic shift in the CT band upon recognition of F^- and CN^- is due to deprotonation of the benzimidazole $-\text{NH}$, as found from the TDDFT calculations of the deprotonated optimized structure of **1** and **4** (Fig. S22, ESI†).



Experimental

Materials and methods

All chemicals and solvents were purchased from commercial sources. 1,2-Diaminoanthraquinone and other reagents were purchased from Sigma-Aldrich and Spectrochem. Solvents are of spectroscopic and GC grade and purchased from Merck. Melting points for the compounds were measured in a SECOR India melting point apparatus and the uncorrected values are reported. UV-visible measurements were performed using a Perkin Elmer lambda 35 spectrophotometer. FT-IR spectra were recorded using a Perkin-Elmer SPECTRUM RX I spectrometer in KBr pellets. ^1H & proton decoupled ^{13}C NMR spectra were recorded using either a JEOL ECS 400 MHz or a Bruker Avance III 500 MHz spectrometer at room temperature and the chemical shifts are reported in parts per million (ppm). Elemental analyses were performed on a Perkin-Elmer 2400 series II CHNS/O series. ESI-MS spectra were recorded using a micromass Q-Tof microTM (Waters) in ESI +ve mode electrospray ionization. The isolated yields were reported for analytically pure compounds.

Syntheses and characterization

General synthetic methods to prepare anthraimidazole-diones. 1,2-Diaminoanthraquinone (1.0 mmol) and different aldehydes (1.0 mmol) were suspended in 60 mL ethanol. Catalytic amounts of trifluoroacetic acid were added to the reaction mixture and heated to reflux for 16 h.^{20,21,94} After completion of the reaction, the reaction mixtures were cooled down to room temperature followed by addition of diethyl ether which led to precipitation of the desired compounds. The precipitates were collected by filtration and washed several times with diethyl ether. Finally the precipitates were collected after drying over P_2O_5 .

2-(2,5-Dihydroxyphenyl)-1H-anthra[1,2-d]imidazole-6,11-dione (1). Dark red solid; Yield 76%; m.p. 235–245 °C (dec). Anal. Calc. for $\text{C}_{21}\text{H}_{12}\text{N}_2\text{O}_4$: C, 70.78; H, 3.39; N, 7.86%. Found C, 70.13; H, 3.33; N, 7.91%. ^1H -NMR (500 MHz, DMSO- d_6) δ 12.66 (s, 1H, OH), 11.17 (s, 1H, OH), 9.21 (s, 1H, NH), 8.19 (m, 2H, ArH), 8.08 (m, 2H, ArH), 7.89 (d, 2H, J = 3 Hz, ArH), 7.88 (d, 1H, J = 3 Hz, ArH), 6.96 (dd, 1H, J = 5 Hz, ArH), 6.88 (m, 1H, ArH) (Fig. S37, ESI \dagger); ^{13}C -NMR (125 MHz, DMSO- d_6) δ 183.8 (CO), 182.1 (CO) 156.0 (ArC), 150.3 (ArC), 149.5 (ArC), 147.9 (ArC), 134.5 (ArC), 134.2 (ArC), 133.3 (ArC), 132.9 (ArC), 131.8 (ArC), 129.8 (ArC), 127.5 (ArC), 126.8 (ArC), 126.3 (ArC), 124.4 (ArC), 123.3 (ArC), 121.1 (ArC), 120.5 (ArC), 117.9 (ArC), 113.9 (ArC) (Fig. S38, ESI \dagger); UV-vis $\lambda_{\text{max}}/\text{nm}$ ($\epsilon/\text{dm}^3 \text{ mol}^{-1} \text{ cm}^{-1}$) in CH_3CN -DMSO (50 : 1) 266 (44068), 319 (13530), 424 (12692). IR (KBr, cm^{-1}) 3391 (s), 2358 (s), 1668 (s), 1495 (s), 1330 (s), 1294 (s), 1261 (s), 1218 (m), 717 (s); ESI-MS (CH_3OH), m/z (calc.): 379.21(379.07) [M + Na]⁺.

2-(4-(Bis(2-chloroethyl)amino)phenyl)-1H-anthra[1,2-d]imidazole-6,11-dione (2). Red solid; Yield 68%; m.p. 260–265 °C (dec). Anal. Calc. for $\text{C}_{25}\text{H}_{19}\text{N}_3\text{O}_2\text{Cl}_2$: C, 64.66; H, 4.12; N, 9.05%. Found C, 64.79; H, 4.15; N, 9.12%. ^1H -NMR (500 MHz, DMSO- d_6) δ 12.71 (s, 1H NH), 8.27 (m, 2H, ArH),

8.19 (m, 2H, ArH), 8.01 (m, 2H, ArH), 7.91 (m, 2H, ArH), 6.91 (d, J = 8.5 Hz, 2H, ArH), 3.84 (m, 8H, $\text{CH}_2\text{CH}_2\text{Cl}$) (Fig. S39, ESI \dagger); ^{13}C -NMR (125 MHz, DMSO- d_6) δ 183.2 (CO), 182.1 (CO), 158.2 (ArC), 149.9 (ArC), 148.7 (ArC), 134.3 (ArC), 134.1 (ArC), 133.2 (ArC), 133.1 (ArC), 132.9 (ArC), 129.8 (ArC), 129.7 (ArC), 127.0 (ArC), 126.7 (ArC), 126.1 (ArC), 123.8 (ArC), 123.3 (ArC), 120.9 (ArC), 117.8 (ArC), 116.8 (ArC), 111.5 (ArC), 51.8 (CH_2Cl), 41.1 ($\text{CH}_2\text{CH}_2\text{Cl}$) (Fig. S40, ESI \dagger); UV-vis $\lambda_{\text{max}}/\text{nm}$ ($\epsilon/\text{dm}^3 \text{ mol}^{-1} \text{ cm}^{-1}$) in CH_3CN -DMSO (50 : 1) 266 (34 550), 315 (29 520), 462 (20 190); IR (KBr, cm^{-1}) 3444 (s), 2922 (w), 1660 (s), 1607 (s), 1489 (s), 1326 (s), 1294 (s), 1184 (m), 1008 (w), 719 (s); ESI-MS (CH_3OH), m/z (calc.): 464.33 (464.09) [M + H]⁺.

2-(1H-Imidazol-2-yl)-1H-anthra[1,2-d]imidazole-6,11-dione (3). Dark brown solid; Yield 75%; m.p. 221–229 °C (dec). Anal. Calc. for $\text{C}_{18}\text{H}_{10}\text{N}_4\text{O}_2$: C, 68.79; H, 3.21; N, 17.83%. Found C, 68.88; H, 3.24; N, 17.91%. ^1H -NMR (500 MHz, DMSO- d_6) δ 8.20 (m, 1H, ArH), 8.11 (m, 1H, ArH), 7.95 (br s, 2H, NH), 7.82 (m, 2H, ArH), 7.48 (d, J = 8 Hz, 1H, ArH), 6.79 (d, J = 8 Hz, 1H, ArH), 6.34 (s, 2H, ArH) (Fig. S41, ESI \dagger); ^{13}C -NMR (125 MHz, DMSO- d_6) δ 184.6 (ArC), 180.2 (ArC), 143.6 (ArC), 139.8 (ArC), 134.5 (ArC), 133.6 (ArC), 131.1 (ArC), 126.2 (ArC), 125.9 (ArC), 121.2 (ArC), 120.3 (ArC), 114.1 (ArC), 111.2 (ArC) (Fig. S42, ESI \dagger); UV-vis $\lambda_{\text{max}}/\text{nm}$ ($\epsilon/\text{dm}^3 \text{ mol}^{-1} \text{ cm}^{-1}$) in CH_3CN -DMSO (50 : 1) 260 (36 575), 499 (7574). IR (KBr, cm^{-1}) 3416 (s), 3368 (s), 1667 (s), 1624 (s), 1588 (s), 1531 (s), 1441 (s), 1329 (s), 1301 (s), 1165 (w), 840 (m), 715 (s); ESI-MS (CH_3OH), m/z (calc.): 315.56 (315.09) [M + H]⁺.

2-(4-Methylthiazol-2-yl)-1H-anthra[1,2-d]imidazole-6,11-dione (4). Blackish brown solid; Yield 62%; m.p. 270–275 °C (dec). Anal. Calc. for $\text{C}_{19}\text{H}_{11}\text{N}_3\text{O}_2\text{S}$: C, 66.07; H, 3.21; N, 12.17%. Found C, 66.35; H, 3.28; N, 12.11%. IR (KBr, cm^{-1}) ^1H -NMR (500 MHz, DMSO- d_6) δ 8.20 (d, J = 7 Hz, 1H, ArH), 8.10 (d, J = 7 Hz, 1H, ArH), 7.93 (br s, 1H, NH), 7.81 (t, J = 6.5 Hz 2H, ArH), 7.48 (d, J = 8.5 Hz, 1H, ArH), 6.79 (d, J = 9 Hz, 1H, ArH), 6.33 (br s, 1H, ArH), CH_3 protons obscure in DMSO- d_6 (Fig. S43, ESI \dagger); ^{13}C -NMR (125 MHz, DMSO- d_6) δ 184.5 (ArC), 180.1 (ArC), 143.5 (ArC), 139.7 (ArC), 134.5 (ArC), 133.6 (ArC), 131.2 (ArC), 126.2 (ArC), 126.0 (ArC), 121.5 (ArC), 120.2 (ArC), 114.1 (ArC), 111.7 (ArC) (Fig. S44, ESI \dagger); UV-vis $\lambda_{\text{max}}/\text{nm}$ ($\epsilon/\text{dm}^3 \text{ mol}^{-1} \text{ cm}^{-1}$) in CH_3CN -DMSO (50 : 1) 260 (22 400), 406 (5600), 504 (3100). IR (KBr, cm^{-1}) 3433 (s), 2373 (s), 1665 (s), 1583 (s), 1328 (s), 1293 (s), 1216 (s), 1048 (w), 1005 (m), 714 (s); ESI-MS (CH_3OH), m/z (calc.): 346.17(346.06) [M + H]⁺.

UV-vis titration of 1 and 4 with F^- and CN^-

20 μL of DMSO solution of 1 and 4 (10^{-2} M) were added in 800 μL acetonitrile solution to make the final concentration 25 μM . Acetonitrile solutions of tetrabutylammonium fluoride (TBAF) and tetrabutylammonium cyanide (TBACN) (10^{-3} μM) were added to the solution of 1 and 4 successively. After 2 minutes the UV-vis spectral data were recorded at room temperature.

Determination of binding ratios (Jobs' plot)

1 and 4 were prepared in a DMSO mixture (40 : 1) to achieve 10 $^{-2}$ μM concentration. Likewise TBAF and TBACN solutions



were prepared in the same concentration (10^{-2} μ M) in acetonitrile. Nine sets of sample solutions containing receptors **1** and **4** with F^- and CN^- were prepared in vials varying the mole fraction of **1** or **4** from 0.1 to 0.9. Thus different volumes of the receptor (**1** or **4**) and analyte solution (TBAF or TBACN) were added to vary the mole fraction from 0.1 to 0.9 keeping the total volume same in each case. After shaking the vials for a few minutes, the UV-vis spectra were recorded. The Job's plots were obtained by plotting ΔA vs. mole fraction of **1** or **4**.

¹H and ¹⁹F NMR titrations

Receptor **1** (10.6 mg, 0.01 mmol) was dissolved in $\text{DMSO}-d_6$ (600 μ L) and TBAF (1 M) in $\text{DMSO}-d_6$ was added into the solution of receptor **1**. After shaking the solution for a minute, ¹H NMR spectra were obtained at room temperature. For compounds **3** and **4** the same methods were followed.

Conclusions

The results emphasize that in the detection of F^- and CN^- using anthraimidazolediones the deprotonation of the benzimidazole -NH in the presence of the anion renders the recognition due to the shift of the CT band. We have seen that variation of the donor arm regulates the deprotonation and hence the recognition ability. When the donor arm has thiimidazole or *p*-hydroquinone it was possible to detect F^- and CN^- . However, selectivity for F^- increased in the presence of Cu^{2+} due to its coordinating ability to the receptor and the influence on the deprotonation of the benzimidazole -NH. The detection limit of 0.038 ppm and selectivity for F^- in the case of **4** is encouraging. The results signify that although the NMR studies reveal the formation of HF_2^- in the case of **1**, **3** and **4**, **3** cannot recognize F^- at concentrations similar to **1** and **4**. The UV-vis spectral studies with OH^- to probe the acidity of the benzimidazole -NH show that benzimidazole -NH is most acidic in **4** followed by **1** and relatively much less acidic in **2** and **3**. It should be noted that the formation of HF_2^- may be good evidence to predict the mechanism but does not necessarily comment on the recognition sensitivity. The presence of sulphur in the heterocyclic ring influences the anion recognition properties in a positive fashion at lower concentrations. In fact when we compare the activity of **4** with the rest in the series we also see that the presence of S in the heterocycle helps distinct recognition of F^- from CN^- in the presence of Cu^{2+} .

Acknowledgements

We earnestly acknowledge DST for financial support *via* project no. SB/S1/IC-02/2014. We also thank IISER Kolkata for infra-structural support. A.S. thanks IISER Kolkata for providing the doctoral fellowship. S.B. is thankful to CSIR, India for the research fellowship.

Notes and references

- P. D. Beer and P. A. Gale, *Angew. Chem., Int. Ed.*, 2001, **40**, 486–516.
- R. Martinez-Manez and F. Sancenon, *Chem. Rev.*, 2003, **103**, 4419–4476.
- P. A. Gale and R. Quesada, *Coord. Chem. Rev.*, 2006, **250**, 3219–3244.
- M. Wenzel, J. R. Hiscock and P. A. Gale, *Chem. Soc. Rev.*, 2012, **41**, 480–520.
- P. A. Gale and C. Caltagirone, *Chem. Soc. Rev.*, 2015, **44**, 4212–4227.
- S. Kubik, *Chem. Soc. Rev.*, 2010, **39**, 3648–3663.
- T. S. Snowden and E. V. Anslyn, *Curr. Opin. Chem. Biol.*, 1999, **3**, 740–746.
- P. A. Gale, *Coord. Chem. Rev.*, 2003, **240**, 1.
- D. L. Ozsvath, *Rev. Environ. Sci. Bio/Technol.*, 2009, **8**, 59–79.
- M. Mousny, S. Omelon, L. Wise, E. T. Everett, M. Dumitriu, D. P. Holmyard, X. Banse, J. P. Devogelaer and M. D. Grynpas, *Bone*, 2008, **43**, 1067–1074.
- Y. Yu, W. Yang, Z. Dong, C. Wan, J. Zhang, J. Liu, K. Xiao, Y. Huang and B. Lu, *Fluoride*, 2008, **41**, 134–138.
- O. Fejerskov, F. Manji and V. Baelum, *J. Dent. Res.*, 1990, **69**, 692–700, discussion 721.
- S. Erdal and S. N. Buchanan, *Environ. Health Perspect.*, 2005, **113**, 111–117.
- P. P. Singh, M. K. Barjatiya, S. Dhing, R. Bhatnagar, S. Kothari and V. Dhar, *Urol. Res.*, 2001, **29**, 238–244.
- M. M. Grice, B. H. Alexander, R. Hoffbeck and D. M. Kampa, *J. Occup. Environ. Med.*, 2007, **49**, 722–729.
- R. R. Dash, A. Gaur and C. Balomajumder, *J. Hazard. Mater.*, 2009, **163**, 1–11.
- H. B. Leavesley, L. Li, K. Prabhakaran, J. L. Borowitz and G. E. Isom, *Toxicol. Sci.*, 2008, **101**, 101–111.
- B. Ballantyne, *Fundam. Appl. Toxicol.*, 1983, **3**, 400–408.
- S. Ayoob and A. K. Gupta, *Crit. Rev. Environ. Sci. Technol.*, 2006, **36**, 433–487.
- S. Saha, A. Ghosh, P. Mahato, S. Mishra, S. K. Mishra, E. Suresh, S. Das and A. Das, *Org. Lett.*, 2010, **12**, 3406–3409.
- N. Kumari, S. Jha and S. Bhattacharya, *J. Org. Chem.*, 2011, **76**, 8215–8222.
- T. Gunnlaugsson, M. Glynn, G. M. Tocci, P. E. Kruger and F. M. Pfeffer, *Coord. Chem. Rev.*, 2006, **250**, 3094–3117.
- C. Suksai and T. Tuntulani, *Chem. Soc. Rev.*, 2003, **32**, 192–202.
- V. Kumar, M. P. Kaushik, A. K. Srivastava, A. Pratap, V. Thiruvenkatam and T. N. G. Row, *Anal. Chim. Acta*, 2010, **663**, 77–84.
- L. M. Zimmermann-Dimer and V. G. Machado, *Dyes Pigm.*, 2009, **82**, 187–195.
- G.-Y. Qing, Y.-B. He, Y. Zhao, C.-G. Hu, S.-Y. Liu and X. Yang, *Eur. J. Org. Chem.*, 2006, 1574–1580.
- D. Aldakov and P. Anzenbacher Jr., *J. Am. Chem. Soc.*, 2004, **126**, 4752–4753.

28 R. Nishiyabu and P. Anzenbacher Jr., *J. Am. Chem. Soc.*, 2005, **127**, 8270–8271.

29 J. Yoo, M.-S. Kim, S.-J. Hong, J. L. Sessler and C.-H. Lee, *J. Org. Chem.*, 2009, **74**, 1065–1069.

30 X. He, S. Hu, K. Liu, Y. Guo, J. Xu and S. Shao, *Org. Lett.*, 2006, **8**, 333–336.

31 D. H. Lee, K. H. Lee and J.-I. Hong, *Org. Lett.*, 2001, **3**, 5–8.

32 R. Nishiyabu and P. Anzenbacher Jr., *Org. Lett.*, 2006, **8**, 359–362.

33 C. Suksai and T. Tuntulani, *Top. Curr. Chem.*, 2005, **255**, 163–198.

34 H. Miyaji, W. Sato and J. L. Sessler, *Angew. Chem., Int. Ed.*, 2000, **39**, 1777–1780.

35 V. Amendola, D. Esteban-Gomez, L. Fabbrizzi and M. Licchelli, *Acc. Chem. Res.*, 2006, **39**, 343–353.

36 F. Han, Y. Bao, Z. Yang, T. M. Fyles, J. Zhao, X. Peng, J. Fan, Y. Wu and S. Sun, *Chem. – Eur. J.*, 2007, **13**, 2880–2892.

37 F. D’Souza and O. Ito, *Chem. Commun.*, 2009, 4913–4928.

38 S. E. Garcia-Garrido, C. Caltagirone, M. E. Light and P. A. Gale, *Chem. Commun.*, 2007, 1450–1452.

39 X. Mei and C. Wolf, *Chem. Commun.*, 2004, 2078–2079.

40 J. Cai, B. P. Hay, N. J. Young, X. Yang and J. L. Sessler, *Chem. Sci.*, 2013, **4**, 1560–1567.

41 R. Zadmar and T. Schrader, *J. Am. Chem. Soc.*, 2005, **127**, 904–915.

42 M. Jablonski and A. J. Sadlej, *J. Phys. Chem. A*, 2007, **111**, 3423–3431.

43 R. D. Falcone, N. M. Correa, M. A. Biasutti and J. J. Silber, *Langmuir*, 2000, **16**, 3070–3076.

44 W.-X. Liu and Y.-B. Jiang, *Org. Biomol. Chem.*, 2007, **5**, 1771–1775.

45 X. Peng, Y. Wu, J. Fan, M. Tian and K. Han, *J. Org. Chem.*, 2005, **70**, 10524–10531.

46 G. Cooke and V. M. Rotello, *Chem. Soc. Rev.*, 2002, **31**, 275–286.

47 S. L. Wiskur, H. Ait-Haddou, J. J. Lavigne and E. V. Anslyn, *Acc. Chem. Res.*, 2001, **34**, 963–972.

48 M. Comes, G. Rodriguez-Lopez, M. D. Marcos, R. Martinez-Manez, F. Sancenon, J. Soto, L. A. Villaescusa, P. Amoros and D. Beltran, *Angew. Chem., Int. Ed.*, 2005, **44**, 2918–2922.

49 M. Comes, E. Aznar, M. Moragues, M. D. Marcos, R. Martinez-Manez, F. Sancenon, J. Soto, L. A. Villaescusa, L. Gil and P. Amoros, *Chem. – Eur. J.*, 2009, **15**, 9024–9033.

50 M. Comes, M. D. Marcos, R. Martinez-Manez, F. Sancenon, J. Soto, L. A. Villaescusa and P. Amoros, *Chem. Commun.*, 2008, 3639–3641.

51 E. J. O’Neil and B. D. Smith, *Coord. Chem. Rev.*, 2006, **250**, 3068–3080.

52 S. Khatua, S. H. Choi, J. Lee, K. Kim, Y. Do and D. G. Churchill, *Inorg. Chem.*, 2009, **48**, 2993–2999.

53 K. Ghosh, A. R. Sarkar, A. Samadder and A. R. Khuda-Bukhsh, *Org. Lett.*, 2012, **14**, 4314–4317.

54 T. Zhang and E. V. Anslyn, *Org. Lett.*, 2006, **8**, 1649–1652.

55 M. M. Linn, D. C. Poncio and V. G. Machado, *Tetrahedron Lett.*, 2007, **48**, 4547–4551.

56 X. Lou, D. Ou, Q. Li and Z. Li, *Chem. Commun.*, 2012, **48**, 8462–8477.

57 B. T. Nguyen and E. V. Anslyn, *Coord. Chem. Rev.*, 2006, **250**, 3118–3127.

58 S.-J. Hong, J. Yoo, S.-H. Kim, J. S. Kim, J. Yoon and C.-H. Lee, *Chem. Commun.*, 2009, 189–191.

59 H. J. Kim, K. C. Ko, J. H. Lee, J. Y. Lee and J. S. Kim, *Chem. Commun.*, 2011, **47**, 2886–2888.

60 J. Du, M. Hu, J. Fan and X. Peng, *Chem. Soc. Rev.*, 2012, **41**, 4511–4535.

61 R. Martinez-Manez and F. Sancenon, *Coord. Chem. Rev.*, 2006, **250**, 3081–3093.

62 H. Lu, Q. Wang, Z. Li, G. Lai, J. Jiang and Z. Shen, *Org. Biomol. Chem.*, 2011, **9**, 4558–4562.

63 J. Isaad and F. Salauen, *Sens. Actuators, B*, 2011, **157**, 26–33.

64 V. Amendola, L. Fabbrizzi and L. Mosca, *Chem. Soc. Rev.*, 2010, **39**, 3889–3915.

65 Y. Wu, X. Peng, J. Fan, S. Gao, M. Tian, J. Zhao and S. Sun, *J. Org. Chem.*, 2007, **72**, 62–70.

66 R. M. Duke, J. E. O’Brien, T. McCabe and T. Gunnlaugsson, *Org. Biomol. Chem.*, 2008, **6**, 4089–4092.

67 K. Okamoto, T. Yamamoto, M. Akita, A. Wada and T. Kanbara, *Organometallics*, 2009, **28**, 3307–3310.

68 S. Nishizawa, R. Kato, T. Hayashita and N. Teramae, *Anal. Sci.*, 1998, **14**, 595–597.

69 Z. Xu, N. J. Singh, S. K. Kim, D. R. Spring, K. S. Kim and J. Yoon, *Chem. – Eur. J.*, 2011, **17**, 1163–1170.

70 Y. Cui, H.-J. Mo, J.-C. Chen, Y.-L. Niu, Y.-R. Zhong, K.-C. Zheng and B.-H. Ye, *Inorg. Chem.*, 2007, **46**, 6427–6436.

71 Z. Xu, S. K. Kim, S. J. Han, C. Lee, G. Kociok-Kohn, T. D. James and J. Yoon, *Eur. J. Org. Chem.*, 2009, 3058–3065.

72 T. Ghosh, B. G. Maiya and M. W. Wong, *J. Phys. Chem. A*, 2004, **108**, 11249–11259.

73 H.-T. Niu, D. Su, X. Jiang, W. Yang, Z. Yin, J. He and J.-P. Cheng, *Org. Biomol. Chem.*, 2008, **6**, 3038–3040.

74 Z. Xu, K. Kim Sook and J. Yoon, *Chem. Soc. Rev.*, 2010, **39**, 1457–1466.

75 C. Marin-Hernandez, L. E. Santos-Figueroa, M. E. Moragues, M. M. M. Raposo, R. M. F. Batista, S. P. G. Costa, T. Pardo, R. Martinez-Manez and F. Sancenon, *J. Org. Chem.*, 2014, **79**, 10752–10761.

76 P. Piatek and J. Jurczak, *Chem. Commun.*, 2002, 2450–2451.

77 M. Querol, J. W. Chen, R. Weissleder and A. Bogdanov Jr., *Org. Lett.*, 2005, **7**, 1719–1722.

78 Y. Zhang and S. Jiang, *Org. Biomol. Chem.*, 2012, **10**, 6973–6979.

79 P. A. Gale, *Chem. Commun.*, 2008, 4525–4540.

80 A. K. Mahapatra, G. Hazra and P. Sahoo, *Beilstein J. Org. Chem.*, 2010, **6**(12), 1–8.

81 R. J. T. Houk, S. L. Tobey and E. V. Anslyn, *Top. Curr. Chem.*, 2005, **255**, 199–229.



82 D. H. Lee, J. H. Im, S. U. Son, Y. K. Chung and J.-I. Hong, *J. Am. Chem. Soc.*, 2003, **125**, 7752–7753.

83 R. M. Duke, E. B. Veale, F. M. Pfeffer, P. E. Kruger and T. Gunnlaugsson, *Chem. Soc. Rev.*, 2010, **39**, 3936–3953.

84 D. Cui, X. Qian, F. Liu and R. Zhang, *Org. Lett.*, 2004, **6**, 2757–2760.

85 P. Mukhopadhyay, Y. Iwashita, M. Shirakawa, S.-i. Kawano, N. Fujita and S. Shinkai, *Angew. Chem., Int. Ed.*, 2006, **45**, 1592–1595.

86 X. Zhang, L. Guo, F.-Y. Wu and Y.-B. Jiang, *Org. Lett.*, 2003, **5**, 2667–2670.

87 N. Sakai, J. Mareda, E. Vauthey and S. Matile, *Chem. Commun.*, 2010, **46**, 4225–4237.

88 P. Anzenbacher Jr., *Top. Heterocycl. Chem.*, 2010, **24**, 205–235.

89 M. V. R. Raju and H.-C. Lin, *Org. Lett.*, 2013, **15**, 1274–1277.

90 A. J. Evans, S. E. Matthews, A. R. Cowley and P. D. Beer, *Dalton Trans.*, 2003, 4644–4650.

91 P. A. Gale, M. B. Hursthouse, M. E. Light, J. L. Sessler, C. N. Warriner and R. S. Zimmerman, *Tetrahedron Lett.*, 2001, **42**, 6759–6762.

92 X. H. Sun, W. Li, P. F. Xia, H.-B. Luo, Y. Wei, M. S. Wong, Y.-K. Cheng and S. Shuang, *J. Org. Chem.*, 2007, **72**, 2419–2426.

93 P. Anzenbacher Jr., K. Jursikova and J. L. Sessler, *J. Am. Chem. Soc.*, 2000, **122**, 9350–9351.

94 R. M. F. Batista, S. P. G. Costa and M. M. M. Raposo, *J. Photochem. Photobiol. A*, 2013, **259**, 33–40.

95 K. Yoshida, T. Mori, S. Watanabe, H. Kawai and T. Nagamura, *J. Chem. Soc., Perkin Trans. 2*, 1999, 393–398.

96 J. Shao, Y. Qiao, H. Lin and H. Lin, *J. Fluoresc.*, 2009, **19**, 183–188.

97 R. M. F. Batista, E. Oliveira, S. P. G. Costa, C. Lodeiro and M. M. M. Raposo, *Org. Lett.*, 2007, **9**, 3201–3204.

98 D. Mondal, M. Bar, D. Maity and S. Baitalik, *J. Phys. Chem. C*, 2015, **119**, 25429–25441.

99 A. Kovalchuk, J. L. Bricks, G. Reck, K. Rurack, B. Schulz, A. Szumna and H. Weisshoff, *Chem. Commun.*, 2004, 1946–1947.

100 C.-Y. Chen, J.-H. Ho, S.-L. Wang and T.-I. Ho, *Photochem. Photobiol. Sci.*, 2003, **2**, 1232–1236.

101 D. Jimenez, R. Martinez-Manez, F. Sancenon and J. Soto, *Tetrahedron Lett.*, 2002, **43**, 2823–2825.

102 D. A. Jose, D. K. Kumar, B. Ganguly and A. Das, *Org. Lett.*, 2004, **6**, 3445–3448.

103 F.-y. Wu, M.-h. Hu, Y.-m. Wu, X.-f. Tan, Y.-q. Zhao and Z.-j. Ji, *Spectrochim. Acta, Part A*, 2006, **65A**, 633–637.

104 H. Miyaji and J. L. Sessler, *Angew. Chem., Int. Ed.*, 2001, **40**, 154–157.

105 P. Anzenbacher Jr., M. A. Palacios, K. Jursikova and M. Marquez, *Org. Lett.*, 2005, **7**, 5027–5030.

106 K. Wannajuk, M. Jamkatoke, T. Tuntulani and B. Tomapatanaget, *Tetrahedron*, 2012, **68**, 8899–8904.

107 S. Anbu, S. Shanmugaraju, R. Ravishankaran, A. A. Karande and P. S. Mukherjee, *Dalton Trans.*, 2012, **41**, 13330–13337.

108 P. B. Maithani, R. Gurjar, R. Banerjee, B. K. Balaji, S. Ramachandran and R. Singh, *Curr. Sci.*, 1998, **74**, 773–777.

109 C. B. Rosen, D. J. Hansen and K. V. Gothelf, *Org. Biomol. Chem.*, 2013, **11**, 7916–7922.

110 P. M. Tolstoy, S. N. Smirnov, I. G. Shenderovich, N. S. Golubev, G. S. Denisov and H.-H. Limbach, *J. Mol. Struct.*, 2004, **700**, 19–27.

111 S.-Y. Chung, S.-W. Nam, J. Lim, S. Park and J. Yoon, *Chem. Commun.*, 2009, 2866–2868.

112 X. Chen, S.-W. Nam, G.-H. Kim, N. Song, Y. Jeong, I. Shin, S. K. Kim, J. Kim, S. Park and J. Yoon, *Chem. Commun.*, 2010, **46**, 8953–8955.

113 X. Lou, L. Zhang, J. Qin and Z. Li, *Chem. Commun.*, 2008, 5848–5850.

114 H. S. Jung, J. H. Han, Z. H. Kim, C. Kang and J. S. Kim, *Org. Lett.*, 2011, **13**, 5056–5059.

